

# Theoretical Investigation of Highly Birefringent All-Solid Photonic Bandgap Fiber With Elliptical Cladding Rods

X. Yu, M. Yan, L. W. Luo, and P. Shum

**Abstract**—We theoretically study for the first time the waveguiding properties of an all-solid photonic bandgap fiber with elliptical cladding rods. High birefringence in the order of  $10^{-3}$  is easily achievable in such fibers. The contributions of the cladding rod's ellipticity, the lattice ratio of the cladding microstructure as well as the index contrast of two soft glasses to the birefringence are systematically evaluated. The evolutions of birefringence with the structure and material variations show that our highly birefringent fiber design can be tailored.

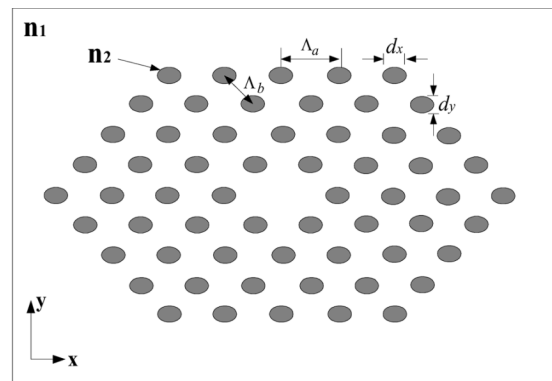
**Index Terms**—Birefringence, photonic bandgap fiber (PBGF), photonic crystal (PC), photonic crystal fiber (PCF).

## I. INTRODUCTION

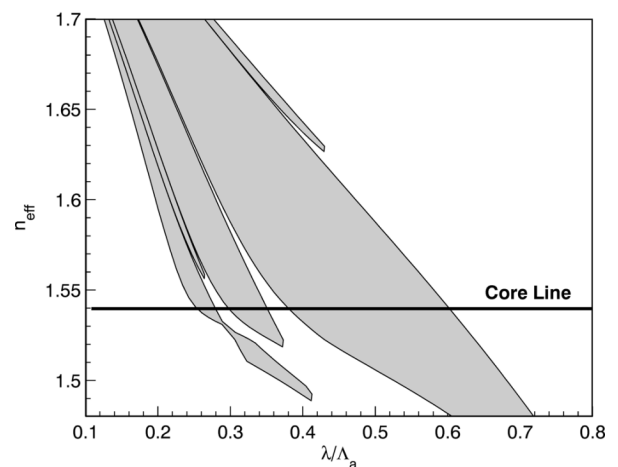
**H**IGHLY birefringent (Hi-Bi) single-mode fiber allows light propagating with preferred polarization direction. Such fiber can be employed for various polarization-sensitive applications, e.g., interferometry, polarization-mode dispersion measurement, sensing, etc. Birefringence can be achieved by intentionally reducing the rotational symmetry of the fiber structure (especially the core structure). Such birefringence is called form birefringence. This type of birefringence effect is more obvious if the core-cladding index contrast is high. Since the advent of air-silica photonic crystal fibers (PCFs), research on form birefringence has thrived [1]–[4], partly due to the fact that symmetry of the core can be easily broken in such high index-contrast microstructured fibers.

The PCFs introduced in [1]–[4] are of index-guiding type. Air-guiding photonic bandgap fiber (PBGF) which has a  $C_{2v}$  rotational symmetry was theoretically investigated in [5]. A later experiment attempt even demonstrated group birefringence as high as  $2.5 \times 10^{-2}$  around  $1.55\text{-}\mu\text{m}$  wavelength in such fiber [6]. An advantage of PBGF is their low bending loss. However, such hollow-core Hi-Bi fiber is not very compatible with existing optical fiber systems though they exhibit high birefringence. Especially, its splicing with conventional single-mode fiber will remain problematic for normal usage. Moreover, distortion of cladding photonic crystal (PC) near core region is inevitable in fabrication of such hollow-core fibers, which is likely to make such fibers suffer from surface modes problem [5].

In this letter, we would like to report a Hi-Bi PBGF design made from high-index rods of elliptical shape isolated in another solid material of low-index. The contributions of elliptical rods,



(a)



(b)

Fig. 1. (a) PBGF with elliptical high-index rod immersed in low-index background material; (b) gapmap of the PC cladding.

lattice ratio, as well as the index contrast to the birefringence are evaluated theoretically. To the best of our knowledge, this is the first demonstration of a Hi-Bi PBGF using high-index elliptical rods in the lattice. Perturbation of cladding PC does not exist in such fiber, hence surface mode problem is eliminated.

## II. Hi-Bi ALL-SOLID PBGF

The cross section of our proposed all-solid Hi-Bi PBGF is shown in Fig. 1(a). It is made of high-index rods ( $n_2$ ) immersed in low-index background material ( $n_1$ ).  $\Lambda_a$ ,  $\Lambda_b$ ,  $d_x$ , and  $d_y$  are the parameters to define the microstructure. Similar nonbirefringent PBGF has recently been reported in [7].  $n_1$  and  $n_2$  are 1.54 and 1.79, respectively. The structure is derived from an equilaterally triangular-latticed PC by compressing it in the  $y$ -direc-

Manuscript received December 27, 2005; revised February 25, 2006.

The authors are with the Network Technology Research Centre, Nanyang Technological University, Singapore 637553, Singapore (e-mail: p145144582@ntu.edu.sg).

Digital Object Identifier 10.1109/LPT.2006.874713

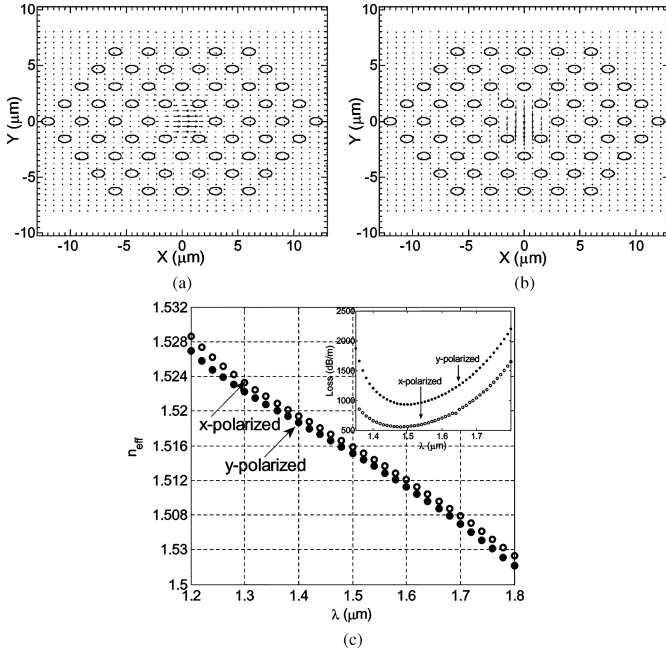


Fig. 2. Transverse electric field of (a)  $HE_{11}^x$ , (b)  $HE_{11}^y$  modes for  $\lambda = 1.55 \mu\text{m}$ ; (c) calculated effective index with varying wavelength for  $HE_{11}^x$  and  $HE_{11}^y$  modes. The inset is the calculated confinement loss.

tion, so that the aspect ratio of a single ellipse is  $d_y/d_x = 0.6$  and the lattice ratio is  $\Lambda_b/\Lambda_a = 0.72$ . The parameters for the fiber are chosen as  $\Lambda_a = 3 \mu\text{m}$ ,  $\Lambda_b = 2.16 \mu\text{m}$ ,  $d_x = 1.125 \mu\text{m}$ ,  $d_y = 0.675 \mu\text{m}$ . The structural compression can be done during fiber drawing, following a technique deployed in [8].

The PC cladding given in Fig. 1(a) exhibits forbidden gaps in the plane-of-periodicity ( $x-y$  plane) when a large propagation constant is assumed in the out-of-plane direction. Such photonic bandgaps are shown in Fig. 1(b), which is calculated using a plane wave expansion method. The wavelength is normalized to the pitch value  $\Lambda_a$ . Notice that the diagram is applicable to PBGFs whose proportion is the same as that shown in Fig. 1(a), but with different scaling factors  $\Lambda_a$  and  $\Lambda_b$  [9]. The largest shaded region is the primary gap region, which will be used in this letter for achieving PBG guidance. It is noticed that the core line ( $n_{\text{eff}} = 1.54$ ) crosses the primary gap region from  $\sim 0.4\Lambda_a$  to  $\sim 0.6\Lambda_a$ . For  $\Lambda_a$  value at  $3 \mu\text{m}$ , we would expect PBG guidance from wavelength  $\sim 1.2$  to  $\sim 1.8 \mu\text{m}$ .

The semivector beam propagation method (SVBPM) is used to calculate the effective mode indexes of the two nondegenerate fundamental modes for the proposed PBGF structure. The parameters used in the SVBPM are as follows: the domain size is  $26 \times 20 \mu\text{m}^2$ , the numbers of grid points along two transverse directions are 260 and 200, and the propagation step size in longitudinal direction is  $0.1 \mu\text{m}$ . Transparent boundary condition is used to enable leaky mode analysis. The  $n_{\text{eff}}$  values of  $HE_{11}^x$  [Fig. 2(a)], and  $HE_{11}^y$  [Fig. 2(b)] modes at  $\lambda = 1.55 \mu\text{m}$  are calculated to be 1.5178 and 1.5169, respectively. Subsequently, by varying the wavelength, we obtain dispersion curves [Fig. 2(c)] and the loss spectrum [Fig. 2(c), inset] for both modes. It can be observed that these effective indexes are less than the refractive indexes of both the cladding rods and the background glass. This confirms the PBG-guiding nature of the waveguide from 1.2 to  $1.8 \mu\text{m}$ . Full-vector finite-difference method (FDM) is used to verify the validity of the BPM results. Comparison of results

TABLE I

COMPARISON OF CALCULATED RESULTS FROM BPM AND FDM AT  $\lambda = 2.0 \mu\text{m}$ 

Method	$n_{\text{eff}}^x$	$n_{\text{eff}}^y$	$B = n_{\text{eff}}^x - n_{\text{eff}}^y$	$L^x$ (dB/m)
BPM	1.489992	1.487556	$2.436 \times 10^{-3}$	3449
FDM	1.490541	1.488083	$2.458 \times 10^{-3}$	4326

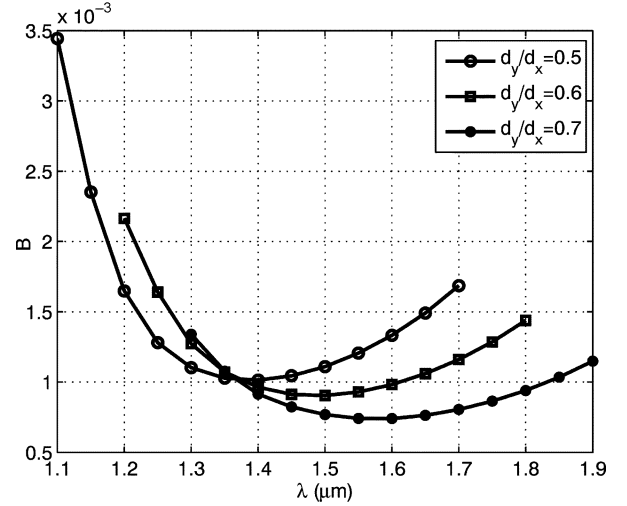


Fig. 3. Calculated birefringence versus wavelength for solid rods with different ellipticity ( $d_y/d_x$ ),  $d_x = 1.125 \mu\text{m}$ ,  $\Lambda_b/\Lambda_a = 0.72$ .

is shown in Table I. The difference of birefringence is around  $2 \times 10^{-5}$ , and the small discrepancy shows good agreement between the two numerical methods.

The confinement loss is calculated to be very high, which is 612 and 978 dB/m for  $HE_{11}^x$  and  $HE_{11}^y$ , respectively, at  $\lambda = 1.55 \mu\text{m}$ . The high confinement loss is due to a small number of cladding rings [10]. The loss for  $HE_{11}^x$  can be reduced to 93 and 19 dB/m when the number of rings in cladding is five and six, respectively. A larger-sized core will also help to improve the confinement. From the inset of Fig. 2(c), we observe that the loss is the lowest in the range from 1.4 to  $1.6 \mu\text{m}$ , which is in agreement with the gapmap. When the operating wavelength goes outside the bandgap, the mode will not be well-confined in the core region and the radiation loss will increase dramatically. It is interesting to notice that the  $x$ -polarized fundamental mode experiences smaller radiation loss than the  $y$ -polarized counterpart. The polarization-dependent loss implies the radiation efficiency is smaller in the  $x$ -direction which might be due to the width of the cladding PC along  $x$ -direction is larger than that along the  $y$ -direction.

The modal birefringence can be calculated for a range of wavelength by:  $B(\lambda) = n_{\text{eff}}^x(\lambda) - n_{\text{eff}}^y(\lambda)$ , where  $n_{\text{eff}}^x$  and  $n_{\text{eff}}^y$  are the effective indexes of  $HE_{11}^x$  and  $HE_{11}^y$  modes, respectively. Numerical calculations in this letter have shown that the birefringence in the proposed PBG fiber can be easily achieved in the order of  $10^{-3}$ . The birefringence value in our calculations is conducted for the whole region of the bandgap and it does not exhibit monotonic variation with wavelength. As shown by the curve with open squares in Fig. 3, the birefringence experiences a decrement with wavelength followed by an increment. This aspect is different from previously reported birefringent PBGFs [5], [11]. The overall birefringence attributes by two factors: the birefringent cladding PC and the core shape. Due to the elliptical

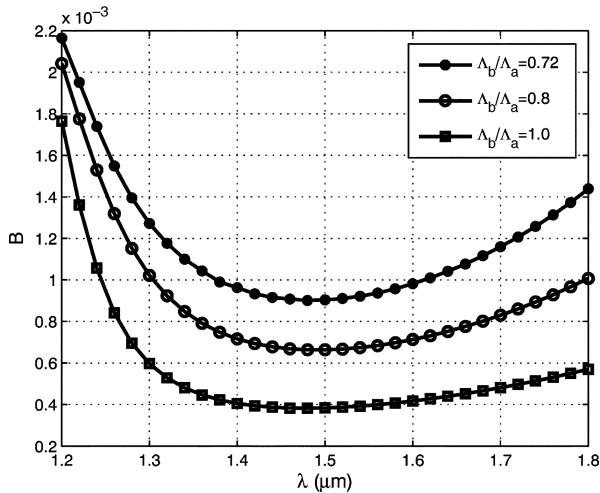


Fig. 4. Calculated birefringence versus wavelength for different lattice ratio ( $\Lambda_b/\Lambda_a$ ),  $\Lambda_a = 3 \mu\text{m}$ ,  $d_y/d_x = 0.6$ .

rods, the PC cladding can be approximated by an anisotropic homogeneous medium. High birefringence at bandgap edges thus can be explained by the large portion of mode distribution into the birefringent cladding. The minimum  $B$  value occurs at the middle of the PBG, as the core mode there is well-confined and the contribution of cladding is minimized. The evolutions of the birefringence are shown in Fig. 3 when we change the ellipticity of the solid rods. The minimum birefringence is increased from  $0.75 \times 10^{-3}$  to  $1 \times 10^{-3}$  when the  $d_y/d_x$  ratio varies from 0.7 to 0.5. Since the lattice ratio is fixed at  $\Lambda_b/\Lambda_a = 0.72$ , so the core shape is not changed significantly. Consequently, the increment of the birefringence is relatively small. PBG-guiding range shifts to a longer wavelength by  $\sim 200$  nm due to change in cladding bandgap. The symmetry of the core, which can be reflected by the cladding lattice ratio  $\Lambda_b/\Lambda_a$ , is another tuning parameter for birefringence. The  $\Lambda_b/\Lambda_a$  is varied from 0.72 to 1.0 by fixing the ellipticity at  $d_y/d_x = 0.6$ ,  $\Lambda_a = 3 \mu\text{m}$ , and the result is shown in Fig. 4. We notice that the birefringence is decreased by half at  $1.55 \mu\text{m}$  when we change our structure in Fig. 1 to an equilaterally triangular-lattice structure. However, the PBG operation region is not shifted much. This is because the bandgap is mostly determined by the shape and index of the high index rods. Other than the contribution of structure asymmetry to the high birefringence, the index contrast in our proposed structure is also expected to have an important impact. Fig. 5 illustrates the decrease of birefringence when varying the index of the high index rods. The birefringence is increased by one order if the index of solid rods is increased from 1.65 to 1.79. Furthermore, the transmission window is red-shifted with the increase of index contrast by more than 400 nm. The evaluations of the impacts of the above factors to high birefringence indicate that our Hi-Bi PBGF can be tailored with great flexibility.

### III. CONCLUSION

We have proposed an all-solid PBGF with elliptical cladding rods. In this structure, there exists a high modal phase birefringence around  $1 \times 10^{-3}$  at  $1.55 \mu\text{m}$ . This property is in-

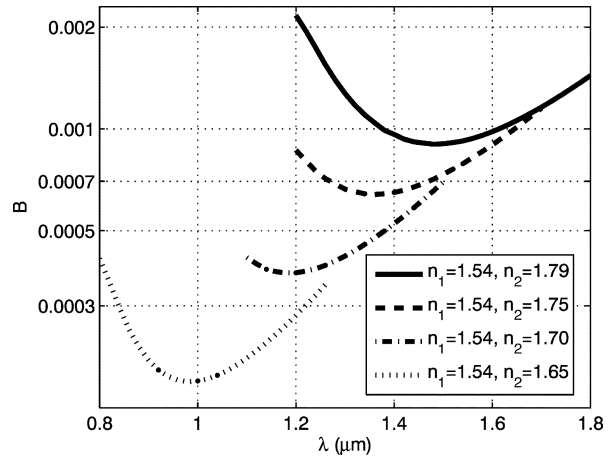


Fig. 5. Calculated birefringence with different high-index rods  $n_2$  for the same fiber structure:  $d_y/d_x = 0.6$ ,  $\Lambda_b/\Lambda_a = 0.72$ .

duced by the reduced rotational symmetry of the fiber structure due to the presence of elliptical rods and different pitch size in the cladding. Moreover, the high index contrast between rods and core material also plays a part in providing the high modal birefringence in the fibers. The identical elliptical shape of high-index rods in cladding eliminates the surface modes problem. The solid core promotes integration with current optical fiber communication devices; while the PBG guidance will allow us to miniaturize the device size owing to the fact the fiber is tolerable to small bending radius.

### REFERENCES

- [1] A. Ortigosa-Blanch, J. C. Knight, W. J. Wadsworth, J. Arriaga, B. J. Mangan, T. A. Birks, and P. S. J. Russell, "Highly birefringent photonic crystal fibers," *Opt. Lett.*, vol. 25, no. 18, pp. 1325–1327, Sep. 2000.
- [2] T. P. Hansen, J. Broeng, S. E. B. Libori, E. Knudsen, A. Bjarklev, J. R. Jensen, and H. Simonsen, "Highly birefringent index-guiding photonic crystal fibers," *IEEE Photon. Technol. Lett.*, vol. 13, no. 6, pp. 588–560, Jun. 2001.
- [3] K. Suzuki, H. Kubota, S. Kawanishi, M. Tanaka, and M. Fujita, "Optical properties of a low-loss polarization—Maintaining photonic crystal fiber," *Opt. Express*, vol. 9, no. 13, pp. 676–680, Dec. 2001.
- [4] H. Kubota, S. Kawanishi, S. Koyanagi, M. Tanaka, and S. Yamaguchi, "Absolutely single polarization photonic crystal fiber," *IEEE Photon. Technol. Lett.*, vol. 16, no. 1, pp. 182–184, Jan. 2004.
- [5] K. Saitoh and M. Koshiba, "Photonic bandgap fibers with high birefringence," *IEEE Photon. Technol. Lett.*, vol. 14, no. 9, pp. 1291–1293, Sep. 2002.
- [6] X. Chen, M.-J. Li, N. Venkataraman, M. T. Gallagher, W. A. Wood, A. M. Vrowley, J. P. Carberry, L. A. Zenteno, and K. W. Koch, "Highly birefringent hollow-core photonic bandgap fiber," *Opt. Express*, vol. 12, no. 16, pp. 3888–3893, Aug. 2004.
- [7] F. Luan, A. K. George, T. D. Hedley, G. J. Pearce, D. M. Bird, J. C. Knight, and P. St. J. Russell, "All-solid photonic bandgap fiber," *Opt. Lett.*, vol. 29, no. 20, pp. 2369–2371, Oct. 2004.
- [8] N. A. Issa, M. A. van Eijkelenborg, M. Fellew, F. Cox, G. Henry, and M. C. J. Large, "Fabrication and study of microstructured optical fibers with elliptical holes," *Opt. Lett.*, vol. 29, no. 12, pp. 1336–1339, Jun. 2004.
- [9] M. Yan, X. Yu, P. Shum, C. Lu, and Y. Zhu, "Honeycomb photonic bandgap fiber with a modified core design," *IEEE Photon. Technol. Lett.*, vol. 16, no. 9, pp. 2051–2053, Sep. 2004.
- [10] K. Saitoh and M. Koshiba, "Confinement losses in air-guiding photonic bandgap fibers," *IEEE Photon. Technol. Lett.*, vol. 15, no. 2, pp. 236–238, Feb. 2003.
- [11] C. Zhang, G. Kai, Z. Wang, Y. Liu, T. Sun, S. Yuan, and X. Dong, "Tunable highly birefringent photonic bandgap fibers," *Opt. Lett.*, vol. 30, no. 20, pp. 2703–2705, Oct. 2005.